Desynchronization Network Analysis for the Recognition of Imagined Movement

Le Song
NICTA and School of Information Technologies
University of Sydney, NSW 2006, Australia
lesong@it.usyd.edu.au

***Abstract*— This paper reports on the use of electroencephalogram (EEG)-based phase desynchronization networks for the recognition of imagined movements. Features derived solely from these networks are classified using linear support vector machine. An average accuracy of 73% is achieved for the single-trial imagined hand versus foot movements. The results demonstrate that phase desynchronizations provide relevant information for the discrimination of mental tasks. This novel approach will potentially benefit the development of brain-computer interfaces.**

I. Introduction

A brain-computer interface (BCI) is a communication system that does not depend on the brain's normal input or output pathways of peripheral nerves [1]. This offers hope for the severely paralyzed to control computers and wheelchairs. The-state-of-the-art of BCIs, however, is still restricted to identifying useful brain signals and designing algorithms to interpret these signals [2].

The most exploited signal for BCIs is the scalp-recorded electroencephalogram (EEG). EEG is a noninvasive measurement of brain activities and has a temporal resolution of milliseconds. A large body of literature have been reported using power spectra, autoregressive model or spatial information for EEG-based BCIs [2]. In this study, a novel approach based on EEG phase desynchronziation networks is introduced for BCIs.

The brain consists of many functionally specialized regions. Dynamic bindings (couplings) of these distributed local neural networks underlie the operation of many mental processes. Phase synchronization has been proposed as a mechanism for this dynamic integration. Phase desynchronization, on the other hand, actively unbinds (uncouples) the neural assemblies and prepares the brain for the next mental state. Evidence suggests that different mental processes are characterized by distinct spatiotemporal patterns of phase dynamics (for a review, see [3]).

Phase synchronization has recently been exploited for BCIs and was shown to contain relevant information for the recognition of mental tasks [4]. The synchronization, however, has been transformed into static values by averaging over space and time. This destroys the spatiotemporal information of the underlying dynamics. In this study, such information is captured by a dynamic network model. Statistics derived solely from these networks are shown to suffice for an accurate classification (>73%) of the single-trial imagined movements. Furthermore, the usefulness of phase desynchronization is also demonstrated for the first time in the context of BCIs.

II. EEG Recording and Experimental Paradigm

The data set investigated in this paper is the data set IVa provided by the Berlin BCI group [5] and is freely available from the BCI competition III web site [6]. For completeness, the recording conditions and experimental paradigm are briefly described.

Recordings were made at 118 positions of the extended international 10/20-system. Signals were band-pass filtered between 0.05 and 200 Hz and then sampled at 100 Hz with 0.1 uV accuracy. Data were collected from five healthy subjects. They were required to imagine they were moving part of their bodies (3.5 s for each imagination) based on the visual cues. Between cues, there were relaxation periods ranging from 1.7 to 2.25 s. Only data for the imagined right hand (class 1) and right foot (class 2) movements are provided in this data set.

III. EEG Desynchronization Networks

EEG signals are processed without re-referencing. Wavelet analysis is used to extract the phase information from each frequency range of interest. The significance of synchronization is then determined for each time point by comparison with the baseline activities. Interestingly, only transient desynchronization can be robustly observed from the data. Dynamic networks are then constructed to capture these transient activities. Details are given in the next three subsections

A. Wavelet-based Phase Locking Statistics (PLS)

EEG signals are well-known for their non-stationarity. Contributions from different frequencies may start and end at different times and their phases usually change over time. Wavelet analysis is well-suited for the analysis of non-stationary signals, due to its excellent temporal resolution even at high frequencies.

Suppose that a signal from electrode i is denoted as $x_i(t)$. The wavelet coefficient $W_i(s,t)$ at scale s and time t is computed using a complex Morlet wavelet [7]. For simplicity, s is henceforth omitted from $W_i(s,t)$.

The instantaneous phase difference $\phi_{ij}(t)$ between $x_i(t)$ and $x_j(t)$ can be computed using their corresponding wavelet

coefficients, i.e.

$$\phi_{ij}(t) = \frac{W_i(t)W_j^*(t)}{|W_i(t)W_j(t)|}, \quad (1)$$

where $\phi_{ij}(t) \in \mathbb{C}$ has unit modulus and all information is contained in the angle. If ϕ_{ij} stays approximately constant over a period of time, x_i and x_j are said to be synchronized; otherwise, they are desynchronized. To quantify this relation, phase locking statistics (PLS) at time t are defined as

$$PLS_{ij}(t) = |\sum_{t-\Delta}^{t+\Delta} \phi_{ij}(t)|, \quad (2)$$

which is the modulus of the sum of $\phi_{ij}(t)$ in a small window $[-\Delta, \Delta]$ centered at t (in practice, $\Delta = 50/f$ where f is the Fourier frequency corresponding to the scale s). $PLS_{ij} \in [0, 1]$, with 0 for complete desynchronization and 1 for perfect synchronization.

Using (1)(2), a PLS is computed for each electrode pair at each time point. The time courses of PLSs are similar across electrode pairs. They are characterized by strong synchronization interwoven with transient bursts of desynchronization, as confirmed by other studies (for an example, see [8]). A typical time course computed at 50 Hz is illustrated in Fig. 1.

The observed synchronization, however, may be spurious, especially for adjacent electrodes. Strong synchronization may result from volume conduction of the brain [7]. The desynchronization, though a more robust observation, can possibly be caused by noise. To resolve these ambiguities, signals from relaxation periods are used.

B. Baseline PLS Distribution

The method of surrogate data is often used to generate a baseline distribution for PLSs [7]. This method, however, does not consider the effect of inter-electrode distance on PLS. Proximal electrode pairs tend to have stronger synchronization than distal pairs. To take this into consideration, the distribution is derived from the relaxation periods instead.

Under a Gaussian assumption, only the mean (μPLS) and standard deviation (σPLS) are computed for each electrode pair. In Fig. 2, a scatter plot of these μPLSs versus inter-electrode distance is illustrated using the data from one subject. This plot clearly reveals the decreasing trend of synchronization as a function of distance. This trend can not possibly be captured by conventional surrogate methods using Gaussian white noise.

C. Desynchronization Networks

Once the baseline distribution is available, significant synchronization and desynchronization can be determined. To be 99% ($p < 0.01$) sure that significant PLSs are not caused by random perturbations, the PLSs are compared to their respective intervals $[\mu PLS - 2.6\sigma PLS, \mu PLS + 2.6\sigma PLS]$. Only those PLSs outside these intervals are significant.

Surprisingly, the overwhelming majority of significant PLSs are due to desynchronization. The pattern is that, at each time point, a subset of electrode pairs desynchronize, and most

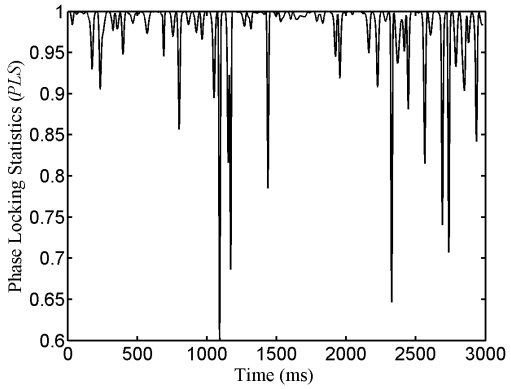

Fig. 1. Typical time course of phase locking statistics for an electrode pair.

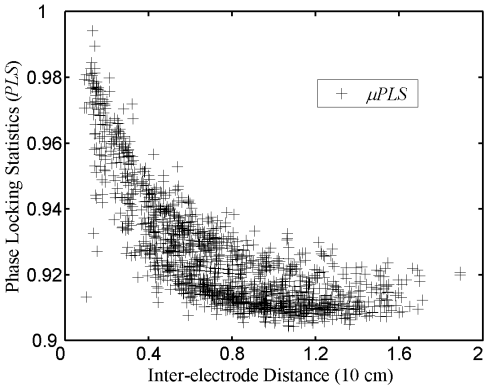

Fig. 2. Baseline phase locking statistics (at 10 Hz) as a function of distance. Each sample point represents an electrode pair.

of these events last for less than 50 ms. These transient inter-electrode relations are supposed to reflect the active unbinding processes in the brain. Averaging the PLSs over space and time, as did in [4], heavily destroys these dynamics. In this study, a dynamic network model is adopted instead to capture these spatiotemporally changing relations.

A dynamic phase desynchronization network is defined as

$$G = \{V, E(t), 1 \le t \le T\}, \quad (3)$$

where $V = \{1, 2, \ldots, 118\}$ is the set of nodes and T is the maximum number of time points in a trial. Each $E(t) = \{e_{ij}(t)\}$ is a set of links at time t, and satisfies $i < j$, $i, j \in V$ and $PLS_{ij}(t) < \mu PLS_{ij} - 2.6\sigma PLS_{ij}$. A dynamic desynchronization network at time t is illustrated in Fig. 3. It is believed that these dynamic networks contain sufficient information for the discrimination of imagined hand versus foot movements.

IV. Features

The features for the discrimination task are based on the probability of link presence (PLP) between two nodes. This feature space is very large (a half of $118 \times 118 \approx 1 \times 10^4$). A criterion is needed to select the most prominent subset of features. To this end, the method of surrogate data is used. The

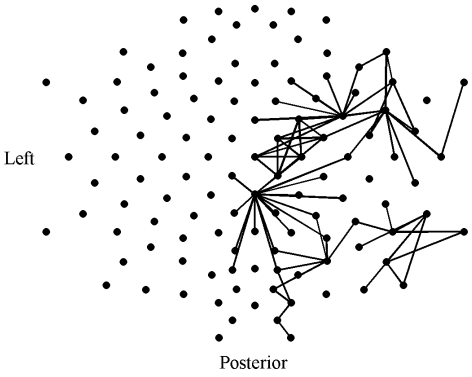

Fig. 3. A desynchronization network at time t. Nodes (representing electrodes) are placed in their positions in the extended international 10/20-system.

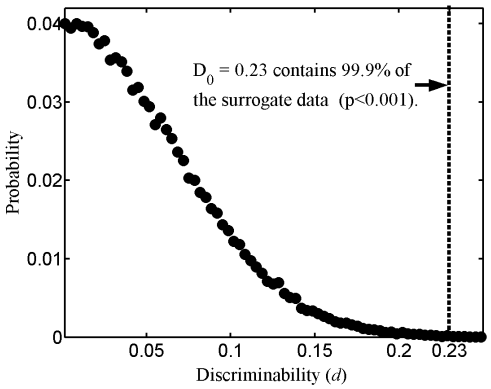

Fig. 4. Distribution of discriminability (d) for $N = 140$.

derived thresholds allow objective selection of those features most beneficial for the classification task.

A. Probability of Link Presence (PLP)

The PLP between node i and j in a desynchronization network G is defined as

$$PLP_{ij} = \frac{\sum_{1 \le t \le T} e_{ij}(t)}{T}. \quad (4)$$

PLP_{ij} is the number of links between i and j, normalized by the total number of time points T. It describes how often desynchronization happens between i and j.

Based on the PLPs from N trials, the mean (μPLP) and standard deviation (σPLP) can be computed for each node pair. Under a Gaussian assumption, the discriminability of the PLP of a node pair for a classification task is defined as

$$d_{ij} = \frac{|\mu PLP^1_{ij} - \mu PLP^2_{ij}|}{\sigma PLP^1_{ij} + \sigma PLP^2_{ij}}, \quad (5)$$

Where the superscripts represent classes (1 or 2) and a higher value of d is desirable. In cases where two classes have independent and identical distribution ($i.i.d.$), a single d of 1 can classify the two classes with an accuracy of 84%. The ds computed from the real networks, however, are generally low, with the majority smaller than 0.4. This means that any single feature alone cannot perform well enough. It is thus necessary to combine several features. In the following subsection, a criterion is derived to choose the useful features.

B. Feature Selection

The low discriminability of the PLPs may caused by inadequate sampling (about a hundred trials for each class) rather than experimental effects. To investigate this issue, two $i.i.d.$ Gaussians are used to generate the surrogate data. Rather than use the μPLPs and σPLPs from the real networks, Gaussians of zero mean and unit standard deviation are used. This is because discriminability is a ratio. It suffices to use the same type of distribution for the random generation.

N (the same as the number of trials) random numbers are generated for each class. Discriminability d is then calculated similarly to (5). After 100,000 realizations of the random generation, a distribution of d is obtained and illustrated in Fig. 4. For different Ns, the distributions are different. Hence, a threshold (D_0) is determined separately for each N. These D_0s are chosen from the tail of the distributions and to be larger than 99.9% ($p < 0.001$) of their respective surrogate data items. All ds from the real networks are then compared against their corresponding D_0s. Only those PLPs satisfying $d > D_0$ are treated as candidate features. This pre-selection excludes the effects of inadequate sampling.

For each subject, there are 140 trials (N=140) for each type of motor imagery, and the dynamic networks are computed for four frequencies $f = 10, 12, 14, 16$ Hz at EEG α and β bands. The threshold used to select features are $D_0 = 0.23$, as illustrated in Fig. 4. For subject 3, the resulting number of candidate features is very small and most of them are highly correlated. His data is henceforth omitted from our further analysis.

V. Classification and Results

Linear support vector machine is used to classify the computed feature vectors from desynchronization networks. Classifiers were trained separately for each subject and 10-fold cross-validation was used to test the generalization ability of the method. The classification accuracies for the four subjects are listed in Table I. The average accuracy for the four subjects is 73%. Notably, for subject 2, an accuracy close to 80% is achieved. This performance is quite satisfactory for this initial attempt to use phase desynchronization networks in BCIs.

TABLE I
Classification Accuracy

Subject	1	2	4	5	Avg. (%)
Class 1 (%)	68.6	80.7	72.9	70.0	73.0
Class 2 (%)	66.4	80.0	72.9	74.3	73.4
Avg. (%)	67.5	80.4	72.9	72.2	73.2

VI. Discussion

Features chosen in this study all have discriminabilities larger than D_0. Under the assumption of a Gaussian and statistical independence, the classification accuracy Q satisfies the inequality [9]

$$Q \geq \frac{1}{\sqrt{2\pi}} \int_{-\infty}^{D_0\sqrt{M}} \exp(\frac{-\upsilon^2}{2}) \mathrm{d}\upsilon, \qquad (6)$$

where M is the number of features. The lower bound for Q increases as the number of features increases.

According to (6), about 68 independent features will give an accuracy of 95% for $D_0 = 0.23$. However, this is far from the case of this study, where typically several hundreds of candidate features are needed to achieve the accuracies listed in Table I. This suggests that many selected features (or equivalent electrode pairs) are correlated.

Furthermore, the selected electrode pairs correspond well to neurophysiological evidence, which suggests that during motor imagery functional couplings occur between the motor cortex of both hemispheres and between lateral and mesial areas of the motor cortex [10]. In Fig. 5, the selected electrode pairs at 12 Hz are illustrated for subject 2. It is clear from the figure that, besides the pattern of couplings as indicated in the literature, functional couplings also occur between the motor cortex and the prefrontal cortex. This may reflect the executive control of the prefrontal cortex over motor imagery.

VII. Conclusion

In this study, the spatiotemporal dynamics of the brain activities are captured by a dynamic phase desynchronization network model. Statistics from the networks are used to classify two types of imagined movements. The average classification accuracy of 73% fits with the evidence from the literature, which suggests that different mental processes are characterized by distinct networks [3]. It is believed that the capacities of the networks have not yet been fully exploited. Further studies on the possible patterns hidden in the networks and the integration of this method with other approaches, such as the method of common spatial patterns [11], have the potential to improve the development of BCIs.

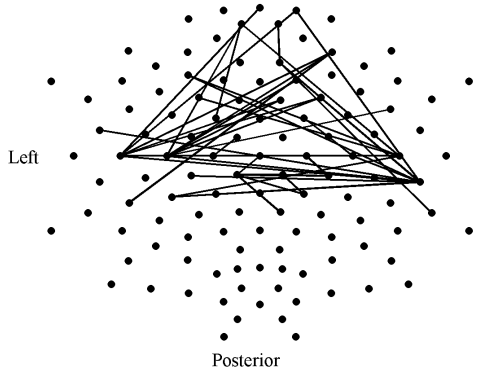

Fig. 5. Selected electrode pairs at 12 Hz show the functional couplings between different areas of the brain. (Experiment data are from subject 2.)

Acknowledgment

The author would like to thank Dr. Julien Epps, Dr. Masahiro Takatsuka, Mr. Colin Murray and Ms. Yingxin Wu from NICTA, and Dr. David Alexander, Dr. Michael Breakspear, Dr. Evian Gordon and Dr. Chris Rennie from Brain Dynamics Center for discussion.

References

[1] J.R. Wolpaw et al., "Brain-computer interface technology: a review of the first international meeting," *IEEE Trans. Rehab. Eng.*, vol. 8, pp. 164-173, 2000.

[2] T.M. Vaughan et al., "Brain-computer interface technonolgy: a review of the second international meeting," *IEEE Trans. Rehab. Eng.*, vol. 11, pp. 94-109, 2003.

[3] F. Varela, J.P. Lachaux, E. Rodriguez, and J. Martinerie, "The brainweb: phase synchronization and large-scale integration," *Nature Reviews Neuroscience*, vol. 2, pp. 229-239, 2001.

[4] E. Gysels, and P. Celka, "Phase synchronization for the recognition of mental tasks in brain-computer interface," *IEEE Trans. Neural Syst. Rehab. Eng.*, vol. 12, pp. 406-415, 2004.

[5] G. Dornhege, B. Blankertz, G. Curio, and K.R. Müller, "Boosting bit rates in non-invasive EEG single-trial classifications by feature combination and multi-class paradigms," *IEEE Trans. Biomed. Eng.*, vol. 51, pp. 993-1002, 2004.

[6] Brain-computer interface competition III web site, `http://ida.first.fraunhofer.de/projects/bci/competition_iii/`.

[7] J.P. Lachaux, E. Rodriguez, J. Martinerie, and F. Varela, "Measuring phase synchrony in brain signals," *Human Brain Mapping*, vol. 8, pp. 194-208, 1999.

[8] M. Breakspear, L. Williams, and C.J. Stam, "A novel method for the topographic analysis of neural activity reveals formation and dissolution of 'dynmaic cell assemblies'," *J. Comput. Neurosci.*, vol. 16, pp. 49-68, 2004.

[9] O. Duda, E. Hart, and G. Stork, *Patttern Classification*, 2^{nd} ed., John Wiley & Sons, 2001.

[10] C. Gerloff et al., "Functional coupling and regional activation of human cortical motor areas during simple, internally paced and externally paced finger movements," *Brain*, vol. 121, pp. 1513-1531, 1998.

[11] H. Ramoser, J. Müller-Gerking, and G. Pfurtscheller, "Optimal spatial filtering of single trial EEG during imagined hand movement," *IEEE Trans. Rehab. Eng.*, vol. 8, pp. 441-446, 2000.